PROCEEDINGS OF SCIENCE

Unstable cosmic-ray nuclei constrain low-diffusion zones in the galactic disk

Hanno Jacobs,[a,*] **Philipp Mertsch**[a] **and Vo Hong Minh Phan**[a]

[a] *Institute for Theoretical Particle Physics and Cosmology (TTK), RWTH Aachen University, 52056 Aachen, Germany*

E-mail: jacobs@physik.rwth-aachen.de, pmertsch@physik.rwth-aachen.de, vhmphan@physik.rwth-aachen.de

Several recent observations in the vicinity of cosmic ray sources hint at a local diffusivity, which is about two to three orders of magnitude lower than the global average. The exact filling fraction of these zones is unclear. We show that secondary to primary and stable to unstable ratios together are sensitive to the presence these zones. We have developed a semi-analytical model of galactic cosmic ray transport with two distinct diffusion regimes, with an on average suppressed value of $\kappa_{\rm disk}$ in the disk compared to the one in the halo, $\kappa_{\rm halo}$ and use this to evaluate the B/C and ^{10}Be/^{9}Be ratios. Making use of preliminary AMS-02 data we find a best fit value of $\kappa_{\rm disk}/\kappa_{\rm halo} = 0.20^{+0.10}_{-0.06}$ with $3.5\,\sigma$. If upcoming HELIX data follow the same trend, the significance could be increased to $6.8\,\sigma$. Adopting a coarse-graining approach, we find the suppression corresponds to filling fraction of $\sim 66\,\%$. We conclude that regions of suppressed diffusion might be larger than usually assumed and ought to be taken into account in models of Galactic cosmic ray transport.

38th International Cosmic Ray Conference (ICRC2023)
26 July - 3 August, 2023
Nagoya, Japan

*Speaker

PoS(ICRC2023)104

1. Introduction

Our fundamental understanding of cosmic ray propagation is based upon the overabundance of certain elements, called *secondaries*, which have been created during the propagation of *primary* cosmic rays by spallation on the interstellar gas [15]. Therefore, secondary to primary ratios allow to determine the traversed matter, called grammage. As the accumulated grammage is three orders of magnitude larger than the column density of the disk, cosmic rays must propagate diffusively, crossing the disc thousands of times. In fact, unstable isotopes allow to constrain the propagation time of these particles. This can be formalised in the standard framework of cosmic rays, where they propagate within a magnetic halo of size H by scattering upon the turbulent magnetic field. The diffusive transport can be characterised by the diffusion coefficient κ [18].

The diffusion coefficient κ is a global parameter, but in fact several recent observations in regions of the disk indicate that the local diffusion coefficient is reduced by two to three orders of magnitude compared to the average. For example around the pulsar wind nebulae Geminga and Monogem the spatial distribution of gamma rays [1, 9], originating from inverse Compton scattering of e^+/e^- pairs at GeV and TeV energies which have been produced by the pulsar, can be explained by a suppressed diffusion coefficient in this region [1]. Additionally, the gamma ray emission from dense molecular clouds in the vicinity of supernova remnants, which is caused by pion production of comic rays accelerated by the supernova remnant hints at a suppression of the diffusion by around two orders of magnitude [14].

The exact extent of these suppression regions remains largely unconstrained, with values ranging from between 25 pc to 100 pc. In the latter case up to 20 % of the disk could be filled by these low diffusion zones. It seems natural to ask whether low diffusion zones may impact galactic cosmic ray transport.

Here, we will devise a simple semi-analytical model of CR propagation in a scenario where we have a suppressed averaged diffusion in the Galactic disk and investigate constraints from upcoming AMS-02 [21] and HELIX [26] $^{10}\mathrm{Be}/^{9}\mathrm{Be}$ measurements. We then show how to calculate a large-scale averaged diffusion coefficient from smaller-scale features using the numerical solution of a stochastic differential equation. Finally, we explain the implications of our findings and conclude.

2. Model

To describe CR propagation in the Galaxy we use a $1D$ diffusion model following Ginzburg & Syrovatskii [18]. Cosmic rays are assumed to propagate in the galactic disk of height $2h$ and a surrounding magnetised halo of size $2H$. The halo has negligible gas density and at the edge a free escape boundary condition is enforced. Both the interstellar gas and the sources are confined within the disk $h \ll H$. It is not possible to analytically solve a model of CR propagation containing spatially resolved zones of suppressed diffusion due to the difference in scales involved. Instead here we resort to a coarse-graining approach, where we have an on average suppressed diffusion coefficient in the disk $\kappa_{\mathrm{disk}}(\mathcal{R})$ compared to the halo $\kappa_{\mathrm{halo}}(\mathcal{R})$ related via

$$\kappa_{\mathrm{disk}}(\mathcal{R}) = \alpha \kappa_{\mathrm{high}}(\mathcal{R}) \quad \text{with} \quad 0 \leq \alpha \leq 1\,. \tag{1}$$

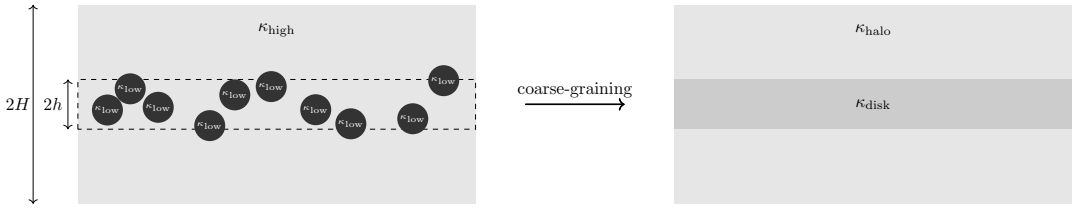

Figure 1: Schematic sketch of low diffusion zones in the disk and the effect of coarse-graining. Zones of low diffusivity $\kappa_{\rm low}$ in the Galactic disk of height $2h$ are surrounded by a zone with high diffusivity $\kappa_{\rm high}$, which extends into the Galactic halo of height $2H$. Coarse-graining leads to an averaged diffusion zone in the disk $\kappa_{\rm disk}$ while in the halo $\kappa_{\rm halo} = \kappa_{\rm high}$.

The rigidity dependence of the diffusion coefficient is modelled as a broken power law to account for spectral breaks observed in CR data at low [30] and high rigidities [10],

$$\kappa(z,\mathcal{R}) = \beta \left(1 + \left(\frac{\mathcal{R}}{\mathcal{R}_l}\right)^{-\frac{1}{s_l}}\right)^{s_l(\delta-\delta_l)} \left(\frac{\mathcal{R}}{10\,\mathrm{GV}}\right)^{\delta} \times \left(1 + \left(\frac{\mathcal{R}}{\mathcal{R}_h}\right)^{\frac{1}{s_h}}\right)^{s_h(\delta_h-\delta)} \times \begin{cases} \kappa_{\rm disk} & z \le h\ , \\ \kappa_{\rm halo} & z > h\ . \end{cases} \tag{2}$$

Some of the parameters have little effect on our results and so we consider values which have been found in other studies. Specifically, we fix $s_l = 0.04$, which has minimal impact on the results, as shown by [31] and the high energy break parameters, which can be determined from primary nuclei [10]: $s_h = 0.5$, $\delta_h = 0.34$, $\mathcal{R}_h = 312\,\mathrm{GV}$. All other parameters remain to be determined by a fit to data. With this diffusion coefficient the steady state transport equation reads[27]:

$$\frac{\partial}{\partial z}\left(v\psi_j - \kappa(z,\mathcal{R})\frac{\partial \psi_j}{\partial z}\right) + \frac{\partial}{\partial p}\left[\left(\frac{\mathrm{d}p}{\mathrm{d}t}\right)\psi_j - \frac{p}{3}\frac{dv}{dz}\psi_j\right] + \frac{1}{\gamma\tau_j}\psi_j + 2h\delta(z)\beta c n_{\rm gas}\sigma_j\psi_j = Q_j(p)\,, \tag{3}$$

where ψ_j is the density differential in momentum of CRs of species j, connected to the phase space density f_j by $\psi_j = 4\pi p^2 f_j$. The terms on the left hand side describe advection, diffusion, (adiabatic) energy losses, decay with boosted decay time $\gamma\tau_j$ and spallation of CRs, respectively. While we distinguish between diffusion at $z < h$ and $z > h$, we neglect the spatial distribution of spallation, energy losses and the sources in the disk, since we expect the effect to be small and approximate them with a delta distribution $\delta(z)$. We make use of the cross sections provided by Evoli et al. [10, 11]. The advection speed $v(z) = \mathrm{sgn}(z)v_c$ is directed vertically out of the Galactic disk and left as a free parameter, giving $\mathrm{d}v/\mathrm{d}z = 2v_c\delta(z)$. The dominating energy loss process is ionisation on neutral gas in the disk, which can again be assumed to be infinitesimal [10, 24]:

$$\left(\frac{\mathrm{d}p}{\mathrm{d}t}\right)_{j,\rm ion} = 2h\dot{p}_j\delta(z)\,, \tag{4}$$

where we use the formula given by Mannheim & Schlickeiser [24] and correct a typo as described in Jacobs et al. [20].

There are three ways to produce CRs of species j, accounted for by the right hand side of eq. (3):

$$Q_j(p) = 2h\delta(z)Q_{{\rm prim},j}(p) + \sum_{k>j}\frac{\psi_k}{\gamma\tau_{k\to j}} + 2h\delta(z)\beta c n_{\rm gas}\sum_{k>j}\sigma_{k\to j}\psi_k\,. \tag{5}$$

The first term describes injection by a population of sources we assume $Q_{\mathrm{prim.}(R)} \propto \mathcal{R}^{-2.3}$ here for all primaries with the abundances given by [11]. Unstable heavier elements can decay into species j, resulting in the second term of (5). Furthermore, heavier CRs can spallate into species j by interacting with the interstellar gas in the disk (the third term of eq. (5)). The uncertainty on those interaction cross-sections will be a source of systematic errors. The disk height is 100 pc and the hydrogen number density is assumed to be $n_{\mathrm{gas}} = 1\,\mathrm{cm}^{-3}$, similar to what was adopted in Ferrière [12], Phan et al. [28].

We solve the above equations in the halo and the disk separately and then connect the two solutions by demanding continuity of both the CR density and flux at the boundary of the regions. For details see **?**]. To account for solar modulation we use a force field model by [19] with a solar modulation potential of $\psi = 700\,\mathrm{MeV}$ that we obtained by a fit to AMS-02 Oxygen data [3]. We use these fluxes to calculate the B/C ratio, where we make the same assumptions as the AMS-02 collaboration on isotopic composition, namely pure ^{12}C as well as a combination of ^{10}B and ^{11}B [2]. These results are fitted to AMS-02 data [2] and recent Voyager data [7]. To break the degeneracy between H and κ_{halo}, which is obtained when only B/C ratios are used, ^{10}Be data are needed, since they allow to determine the propagation time. Because a suppressed diffusion coefficient in the disk inhibits the escape of freshly produced ^{10}Be into the halo, these measurements can also potentially allow to determine α. For kinetic energies per nucleon below a few GeV we use available data presented in Connell [5], Garcia-Munoz et al. [16, 17], Lukasiak [22], Lukasiak et al. [23], Nozzoli & Cernetti [25], Wiedenbeck & Greiner [32], Yanasak et al. [33], and for energies above $E_{k/n} \approx 1\,\mathrm{GeV/n}$ we will consider preliminary AMS-02 data [21]. In addition, we will forecast the constraining power of upcoming HELIX data [26] by fitting to mock data.

In order to find the best-fit parameters we adopt a Gaussian log-likelihood,

$$-2\ln\left(\mathcal{L}(\theta)\right) = \chi^2(\theta) = \sum_{d,i}\left(\frac{O_{d,i} - O_{d,i}^{(m)}(\theta)}{\sigma_{d,i}}\right)^2, \tag{6}$$

where d runs over the observables B/C and ^{10}Be/^{9}Be and i runs over rigidities $\mathcal{R}_i$ for B/C AMS-02 data or kinetic energies per nucleon $E_{k/n,i}$ else. We have refrained from taking into consideration the possibility of correlated errors [see, e.g. 8] as no official information on this has been provided by the collaborations; we also consider this to be of lesser importance than, for instance, in searches for excesses well-localised in rigidity [e.g. 4].

We have performed a Monte Carlo Markov Chain (MCMC) study which also provides robustness in the identification of the best-fit parameter values. We make use of the `emcee` package [13] and use unbiased priors.

In the following we will investigate the null hypothesis, i.e. that there is no suppression, and the full model for different data sets. Each of them contains the AMS-02 and Voyager B/C data, together with all published ^{10}Be/^{9}Be data. The first setup ("w/o prelim.") reflects our best knowledge to date and only accounts for existing data. The second setup ("w/ prelim.") additionally takes into account preliminary AMS-02 data on ^{10}Be/^{9}Be [21]. We expect the latter to be able to break the degeneracy of κ and H. Additionally we will predict the effects of upcoming HELIX data as described above in the setup called "w/o forecast".

3. Results

The results of the MCMC scan are shown in fig. 2, where the best fit point is indicated with black lines. In the $2D$ posterior the 68 % (95 %) quantiles are indicated in blue and in the $1D$ posteriors the 16 % and 84 % quantiles are indicated by blue dashed lines. The $1D$ posterior of α indicates that a suppressed diffusion coefficient is preferred. Furthermore, an anticorrellation between the diffusion coefficient in the scaling factor exists, hence a larger diffusion coefficient in the halo can partially compensate a smaller one in the disk. The degeneracy of $\kappa_{\rm halo}$ and halo height H expected to exist for B/C and low energy Be data is largely broken and the halo height can be constrained to $H = 8.2^{+1.1}_{-0.9}$ kpc. Another clear degeneracy is visible between δ and v_c, which is a known feature of diffusion-advection models, see e.g. Fig. 2 of Putze et al. [29]. A larger advection speed decreases the secondary-to-primary ratio over a limited rigidity range, more at smaller energies than at larger ones, where diffusion becomes dominant. This energy dependence can be compensated by a larger energy dependence of the diffusion coefficient, hence larger δ. For values of δ_l close to δ the position of the break R_l is unconstrained, leading to volume effects as visible in the lowest row of the plot.

To compare models we cannot rely on the posterior of the MCMC scan since it is lacking statistics in the tail as well as being affected by volume effects. Hence, we can estimate the median and its error by the MCMC scan, but use a likelihood ratio test and account for the null hypothesis being at the boundary of our parameter space [6]. This results in a $3.5\,\sigma$ preference for a model with suppressed diffusion. Should the trend continue with upcoming HELIX data, we forecast a detection by $6.8\,\sigma$.

4. Discussion and Conclusion

The suppressed diffusion coefficient in the disk can originate from two different scenarios. Either the suppression is nearly everywhere, for example caused by different turbulence generation and damping processes in the disk, or only in localised regions. Recent non linear galactic transport models, which consider injection of turbulence in the disk due to supernova explosions as well as self-generated turbulence find that the diffusion coefficients is highest in the disk and decreases towards the halo boundary. However, these models do not consider the shape of the galactic magnetic field, which must be important for self generated turbulence. Given that preliminary AMS-02 data prefer a suppressed diffusion coefficient in the disk it would be interesting to revisit these models with a more precise treatment of the magnetic field. For the scenario where the suppressed diffusion coefficient is due to localised bubbles, we have estimated the scaling factor α for a given ratio of $(\kappa_{\rm low}/\kappa_{\rm high})$ by solving the diffusion equation numerically using stochastic differential equations (SDE). We have computed the average diffusion coefficient from the mean-square displacement of particles and checked that the exact geometry of the low diffusion zones does not matter for the asymptotic values, but only the filling fraction. In Fig. 3 we show the scaling factor α as a function of filling fraction. The grey line and zone indicate the values found from the CR fit, which shows that the best fit filling fraction is around ~ 66 %.

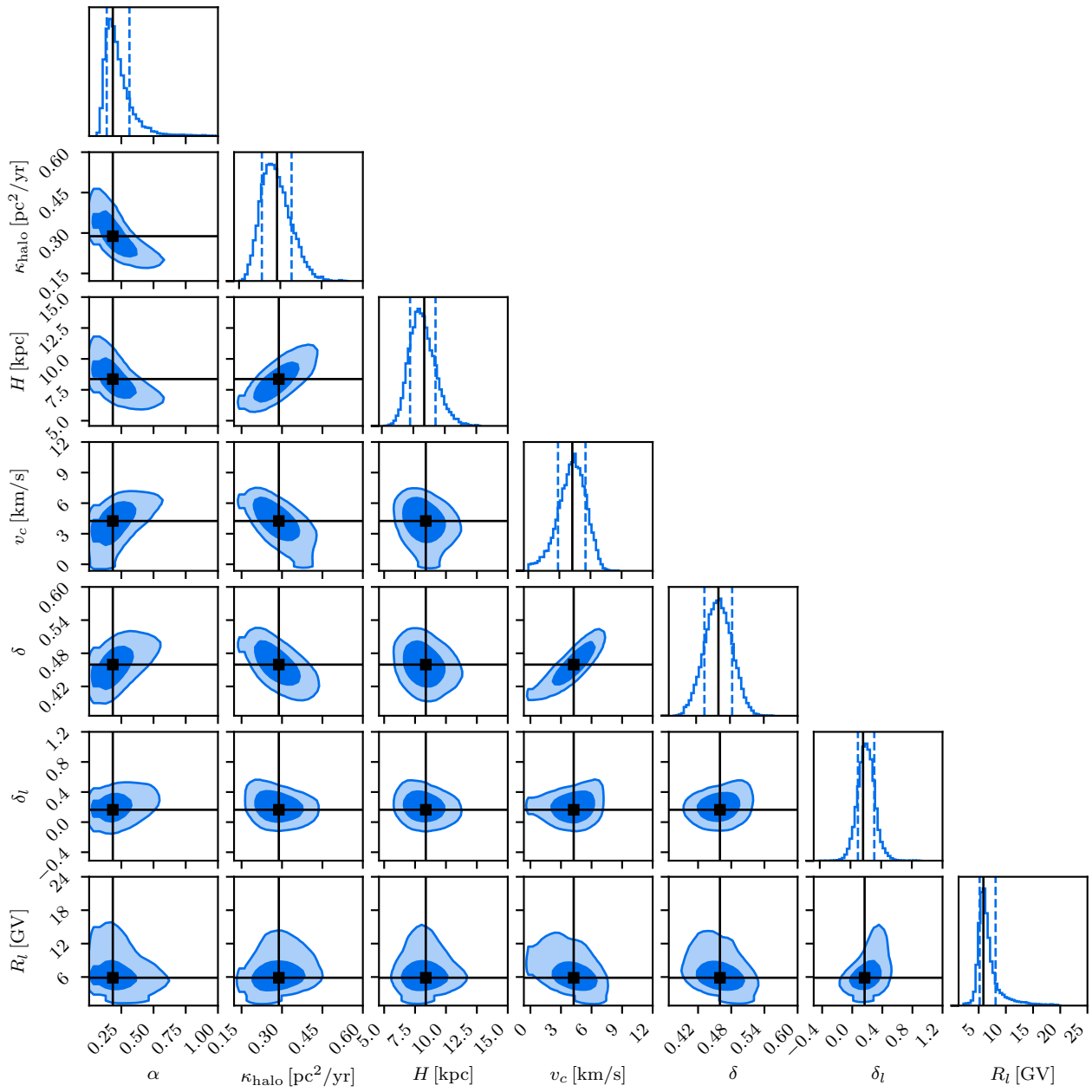

Figure 2: Corner plot of the MCMC scan of the full model including preliminary data, "w/ prelim.". The 2D marginalised posteriors are shown on the lower triangle. The dark/bright blue areas corresponds to the 68 %/95 % quantiles. Similarly, the principal diagonal displays the 1D marginalised posterior with the 16 % and 84 % quantiles marked as blue dashed lines. The black lines indicate the best fit values.

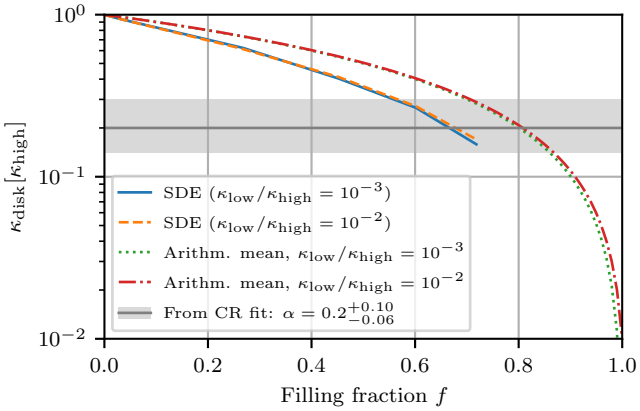

Figure 3: Effective diffusion coefficient $\kappa_{\rm disk}$ from the SDE computation as a function of the volume filling fraction f. The solid blue (dashed orange) line shows $\kappa_{\rm disk}$ in unit of $\kappa_{\rm high}$, assuming a ratio $\kappa_{\rm low}/\kappa_{\rm high}$ of 10^{-3} (10^{-2}). The sources of CRs are assumed to be distributed uniformly in the disk. Note that the lines end at the maximum possible filling fraction of $\sim 74\,\%$ for spherical inclusions. For comparison, the green dotted (red dot-dashed) line shows the arithmetic mean $(\kappa_{\rm low}/\kappa_{\rm high})f + (1-f)$ assuming $\kappa_{\rm low}/\kappa_{\rm high}$ of 10^{-2} (10^{-3}). The grey line and band highlight the suppression found from the CR fit, $\alpha = 0.2^{+0.10}_{-0.06}$.

References

[1] Abeysekara A. U., et al., 2017, Science, 358, 911

[2] Aguilar M., et al., 2016, Phys. Rev. Lett., 117, 231102

[3] Aguilar M., et al., 2021, Phys. Rev. Lett., 126, 041104

[4] Boudaud M., Génolini Y., Derome L., Lavalle J., Maurin D., Salati P., Serpico P. D., 2020, Physical Review Research, 2, 023022

[5] Connell J. J., 1998, ApJ, 501, L59

[6] Cowan G., Cranmer K., Gross E., Vitells O., 2011, European Physical Journal C, 71, 1554

[7] Cummings A. C., et al., 2016, ApJ, 831, 18

[8] Derome L., Maurin D., Salati P., Boudaud M., Génolini Y., Kunzé P., 2019, A&A, 627, A158

[9] Di Mauro M., Manconi S., Donato F., 2019, Phys. Rev. D, 100, 123015

[10] Evoli C., Aloisio R., Blasi P., 2019, Phys. Rev. D, 99, 103023

[11] Evoli C., Morlino G., Blasi P., Aloisio R., 2020, Phys. Rev. D, 101, 023013

[12] Ferrière K. M., 2001, Reviews of Modern Physics, 73, 1031

[13] Foreman-Mackey D., et al., 2013, emcee: The MCMC Hammer, Astrophysics Source Code Library, record ascl:1303.002 (ascl:1303.002)

[14] Gabici S., Casanova S., Aharonian F. A., Rowell G., 2010, in Boissier S., Heydari-Malayeri M., Samadi R., Valls-Gabaud D., eds, SF2A-2010: Proceedings of the Annual meeting of the French Society of Astronomy and Astrophysics. p. 313 (arXiv:1009.5291), doi:10.48550/arXiv.1009.5291

[15] Gabici S., Evoli C., Gaggero D., Lipari P., Mertsch P., Orlando E., Strong A., Vittino A., 2019, International Journal of Modern Physics D, 28, 1930022

[16] Garcia-Munoz M., Mason G. M., Simpson J. A., 1977, ApJ, 217, 859

[17] Garcia-Munoz M., Simpson J. A., Wefel J. P., 1981, in International Cosmic Ray Conference. p. 72

[18] Ginzburg V. L., Syrovatskii S. I., 1964, The Origin of Cosmic Rays

[19] Gleeson L. J., Axford W. I., 1967, ApJ, 149, L115

[20] Jacobs H., Mertsch P., Phan V. H. M., 2022, J. Cosmology Astropart. Phys., 2022, 024

[21] Jiahui Wei 2022, Properties of Cosmic Beryllium Isotopes, URL: https://agenda.infn.it/event/28874/contributions/170166/attachments/93944/128556/ICHEP2022_Be_Isotope.pdf

[22] Lukasiak A., 1999, in 26th International Cosmic Ray Conference (ICRC26), Volume 3. p. 41

[23] Lukasiak A., Ferrando P., McDonald F. B., Webber W. R., 1994, ApJ, 423, 426

[24] Mannheim K., Schlickeiser R., 1994, A&A, 286, 983

[25] Nozzoli F., Cernetti C., 2021, Universe, 7, 183

[26] Park N., et al., 2019, in 36th International Cosmic Ray Conference (ICRC2019). p. 121, doi:10.22323/1.358.0121

[27] Parker E. N., 1965, Planet. Space Sci., 13, 9

[28] Phan V. H. M., Schulze F., Mertsch P., Recchia S., Gabici S., 2021, Phys. Rev. Lett., 127, 141101

[29] Putze A., Derome L., Maurin D., 2010, A&A, 516, A66

[30] Vittino A., Mertsch P., Gast H., Schael S., 2019, Phys. Rev. D, 100, 043007

[31] Weinrich N., et al., 2020, A&A, 639, A74

[32] Wiedenbeck M. E., Greiner D. E., 1980, ApJ, 239, L139

[33] Yanasak N. E., et al., 2001, ApJ, 563, 768